

Note added in proof. Tefft, Bell, and Romero²¹ (TBR) have recently used the same set of orthogonal functions (with minor differences in notation) as used in this work [Eq. (2.5)] to calculate effective-mass binding energies. However, TBR computed only the diagonal elements of the Hamiltonian matrix. The neglect of the off-diagonal matrix elements destroys the central principle of the variational method, namely, that the approximations to the eigenvalues are upper bounds to the true eigen-

²¹ W. E. Tefft, R. G. Bell, and H. V. Romero, *Phys. Rev.* **177**, 1194 (1969).

values in a one-to-one correspondence. This becomes extremely serious when quasidegeneracies occur. Therefore, the results of TBR bear little or no relationship to the true eigenvalues of the effective-mass Hamiltonian except for the ground states of each symmetry ($1S$, $2P_0$, $2P_{\pm}$, etc.).

ACKNOWLEDGMENTS

The authors wish to thank J. J. Hopfield for several useful discussions on this work, and E. O. Kane and P. J. Dean for critical readings of the manuscript.

Spin-Orbit Effects in Crossed Electric and Magnetic Fields; Γ_7 Band of Wurtzite-Type Crystals

KUNIICHI OHTA

I. C. Division, Nippon Electric Company, 1753, Shimonumabe, Kawasaki, Japan

(Received 9 September, 1968; revised manuscript received 18 June 1969)

The Γ_7 conduction band of the wurtzite-type II-VI compounds has a spin-orbit term linear in \mathbf{k} . Effects of this spin-orbit term in crossed electric and magnetic fields are investigated on the basis of a one-band formalism. The effective Hamiltonian is solved for four different cases, according to the strength of the crossed electric and magnetic fields: (A) Strong magnetic field and weak electric field—this is essentially the simple band case; (B) weak magnetic field and weak electric field (the coupling between cyclotron motion and spin states via the spin-orbit term plays a dominant role in determining the energy spectrum); (C) strong magnetic field and strong electric field. (The major contribution to the spin-orbit interaction comes from a term representing the influence of transverse drift motion upon spin states. As a result, the spin splitting exhibits a nearly linear dependence on the electric field, and the direction of the spin axis tends toward that of the electric field with increasing electric field); (D) weak magnetic field and strong electric field [both of the spin-orbit effects, which are predominant either in the case (B) or in the case (C), are equally important, and perturbation theory is not applicable. Variational solutions have amplitudes distributed over many Landau and spin states, so that the selection rule for the intraband transitions is relaxed.] The conditions for observing these spin-orbit effects by means of intraband transitions are discussed for the actual II-VI compounds. It is found that spin-orbit effects may possibly be observed in magnetic dipole transitions under the condition of case C for CdS and ZnS, as well as in electric and magnetic dipole transitions under the condition of case A or C for CdSe. In the strong electric field of case C, the transverse drift velocity is one or two orders of magnitude larger than the velocity of sound in the crystal. Hence, phonon clouds build up around an electron to cause broadening of the resonance line. This can be avoided by carrying out the resonance experiment before the phonon clouds build up, i.e., by employing a pulsed transverse electric field.

I. INTRODUCTION

INVESTIGATION of the electronic states in crossed electric and magnetic fields has given valuable information concerning the band structure of semiconductors. The first theoretical study on this subject was made by Aronov¹ on the basis of a simple band model. The one-band effective Hamiltonian has a simple harmonic solution which can explain many qualitative features of the interband optical transitions. Later, a more appropriate theory based on a two-band model was developed by Lax and co-workers² and also by Aronov,³

¹ A. G. Aronov, *Fiz. Tverd. Tela* **5**, 552 (1963) [English transl.: *Sov. Phys.—Solid State* **5**, 402 (1963)].

² B. Lax, in *Proceedings of the Seventh International Conference on the Physics of Semiconductors Paris, 1964*, edited by M. Hulin (Academic Press Inc., New York, 1964), Vol. I, p. 253; B. Lax,

giving successful explanations of some critical phenomena^{3,4} in the strong crossed electric field.

In the case of a complex band, however, we have to solve a set of differential equations resulting from the effective Hamiltonian.⁵ The only exact solution obtained so far is the one derived by Luttinger⁶ for the valence band of germanium or silicon in a magnetic field along the [111] direction with no electric field. When a weak electric field is applied perpendicular to the magnetic

J. Phys. Soc. Japan Suppl. **21**, 165 (1966). The latter is a review article in which an extensive list of references is given.

³ A. G. Aronov, *J. Phys. Soc. Japan Suppl.* **21**, 608 (1966).

⁴ W. Zawadzki and B. Lax, *Phys. Rev. Letters* **16**, 100 (1966).

⁵ E. I. Blount, in *Solid State Physics*, edited by F. Seitz and D. Turnbull (Academic Press Inc., New York, 1962), Vol. 13, p. 306.

⁶ J. M. Luttinger, *Phys. Rev.* **102**, 1030 (1956).

field, one observes a small energy shift of the Landau levels which can be treated by perturbation theory.⁷

Most of the II-VI compounds with wurtzite structure have their conduction and valence-band extrema at the Γ point ($\mathbf{k}=0$), and their assignment to the Γ_7 conduction and $\Gamma_9(A)$, $\Gamma_7(B)$, and $\Gamma_7(C)$ valence bands has been almost established by the detailed studies of exciton spectra.⁸ The one-band effective-mass Hamiltonian has the form of a simple band with an anisotropic effective mass and g factor. According to group theory,⁹ there is a spin-orbit term linear in \mathbf{k} in the Γ_7 band. This spin-orbit coupling term arises from the combined effect of spin-orbit coupling and crystal field, as is shown by $\mathbf{k}\cdot\mathbf{P}$ perturbation theory for the original one-electron Hamiltonian. Owing to the presence of this spin-orbit term, the energy spectrum of the Γ_7 band has an extremum loop in a plane normal to the Γ - Δ - A axis. The effect of this spin-orbit term on the $\Gamma_7(B)$ band has been investigated for CdS by the interband magneto-optical absorption¹⁰ and by the anomalous reflection spectra of exciton.¹¹ Thus, the coefficient of the spin-orbit term (denoted by C) was determined experimentally for the $\Gamma_7(B)$ band of CdS. However, no attempt has successfully been made so far for the determination of the spin-orbit parameter C for the Γ_7 conduction band.

The purpose of this paper is to show that, in the case of the Γ_7 conduction band, the application of crossed electric and magnetic fields¹² will be a valuable tool for the determination of the spin-orbit parameter C . Since no experimental confirmation has been achieved, an attempt has been made to put the results in a form which may readily be compared with the experimental results for the actual II-VI compounds. It is hoped that the possibility of observing the spin-orbit effects will be verified by experimental studies along the line described in this paper.

We introduce, in Sec. II, a one-band effective Hamiltonian⁹ for the Γ_7 band in crossed magnetic (along the c axis) and electric (normal to the c axis) fields and reduce it in a convenient form for later calculations. In Sec. III, we solve the Hamiltonian in some limiting cases to obtain analytical expressions for its eigenvalues. It is found that these eigenvalues depend upon the electric and magnetic fields, and also parametrically upon the value of C . Then one can determine the value of C by fitting the electric and magnetic field dependence of the eigenvalues to experiment. In Sec. IV, intraband electric and magnetic dipole transitions are discussed.

Owing to the presence of the spin-orbit term, there are many additional electric and magnetic dipole transitions other than those of cyclotron and spin resonance, respectively. Intensities of these additional transitions, contrary to those of cyclotron or spin resonance ones, depend critically upon the value of C . In Sec. V, the spin-orbit parameter C for the wurtzite-type CdS, CdSe, and ZnS are estimated from the known band parameters on the basis of quasicubic model.^{9,13} A more subtle estimate for CdS is derived from the value of C ^{9,11} for the Γ_7 valence band which was obtained by the analysis of anomalous reflection spectra of exciton. On the basis of these estimates, conditions for observing the spin-orbit effects on the Γ_7 conduction band are discussed for CdS, CdSe, and ZnS. In Sec. VI, summary and conclusions are given.

II. ONE-BAND EFFECTIVE HAMILTONIAN

The behavior of an electron in the Γ_7 band in crossed electric and magnetic fields is investigated within the framework of a one-band effective Hamiltonian. We shall confine ourselves to the case of intraband transitions where the crossed electric and magnetic fields have moderate strength. The conditions necessary for the one-band effective Hamiltonian to be valid have already been discussed by Zak and Zawadzki.¹⁴ These conditions are assumed to be satisfied here. In a magnetic field H directed along the c axis (which is taken as the z axis) and an electric field E along the y axis, the effective Hamiltonian⁹ for the Γ_7 band may be written in the form

$$\mathcal{H} = \frac{\hbar^2}{2m_1}(\kappa_x^2 + \kappa_y^2) + (\hbar^2/2m_1)\kappa_z^2 + C(\kappa_x\sigma_y - \kappa_y\sigma_x) + \frac{1}{2}g_1\beta H\sigma_z + eEy. \quad (1)$$

Here, σ_x , σ_y and σ_z are Pauli spin matrices; $\boldsymbol{\kappa} = -i\mathbf{A} + (e/c\hbar)\mathbf{A}$; $\mathbf{A} = (-Hy, 0, 0)$; C is the coefficient of the spin-orbit term; and other definitions are as in conventional use. κ_x and κ_y satisfy the following commutation relations:

$$[\kappa_x, \kappa_y] = -i(eH/c\hbar) = -i\kappa^2, \quad (2a)$$

$$[\kappa_y, \kappa_z] = [\kappa_x, \kappa_z] = 0. \quad (2b)$$

In our gauge for the vector potential, we can take a plane-wave representation for the motion along the x and z axes, regarding the operators $-i\partial/\partial x$ and $-i\partial/\partial z$ as scalars k_x and k_z . Eliminating y by the relation $y = (k_x - \kappa_x)/\kappa^2$ and introducing operators a and a^\dagger defined by

$$a = \frac{1}{\sqrt{2\kappa}} \left[\kappa_y + i \left(\kappa_x - \frac{m_1 c E}{\hbar H} \right) \right], \quad (3a)$$

⁷ Q. H. F. Vreken, W. Zawadzki, and M. Reine, Phys. Rev. **158**, 702 (1967); T. Shindo, Phys. Chem. Solids **26**, 1431 (1965).

⁸ *Physics and Chemistry of II-VI Compounds*, edited by M. Aven and J. S. Prener (North-Holland Publishing Co., Amsterdam, 1967); *II-VI Semiconducting Compounds*, edited by D. G. Thomas (W. A. Benjamin, Inc., New York, 1967).

⁹ J. J. Hopfield, J. Appl. Phys. Suppl. **32**, 2277 (1961); R. C. Casella, Phys. Rev. **114**, 1514 (1959).

¹⁰ E. Hanamura, Phys. Letters **13**, 116 (1964).

¹¹ G. D. Mahan and J. J. Hopfield, Phys. Rev. **135**, A428 (1964).

¹² K. Ohta, Phys. Letters **17**, 91 (1965).

¹³ J. J. Hopfield, Phys. Chem. Solids **15**, 97 (1960).

¹⁴ J. Zak and W. Zawadzki, Phys. Rev. **145**, 536 (1966).

$$a^\dagger = \frac{1}{\sqrt{2}\kappa} \left[\kappa_y - i \left(\kappa_x - \frac{m_1 c E}{\hbar H} \right) \right], \quad (3b)$$

the Hamiltonian can be rewritten as

$$\begin{aligned} \mathcal{H} = & \hbar\omega_c \{a, a^\dagger\} + \frac{1}{2} g_{11} \beta H \sigma_z \\ & - C \left[\sigma_+ \left(\sqrt{2}\kappa a + i \frac{m_1 c E}{\hbar H} \right) + \sigma_- \left(\sqrt{2}\kappa a^\dagger - i \frac{m_1 c E}{\hbar H} \right) \right] \\ & + \frac{\hbar^2}{2m_{11}} k_z^2 + \hbar k_x \frac{cE}{H} - m_1 \left(\frac{cE}{H} \right)^2, \quad (4) \end{aligned}$$

where

$$\{a, a^\dagger\} = \frac{1}{2}(aa^\dagger + a^\dagger a), \quad \sigma_\pm = \frac{1}{2}(\sigma_x \pm i\sigma_y)$$

and

$$\omega_c = eH/m_1 c.$$

Let us denote the base vector by $|nk_x k_z \pm\rangle$, which is diagonal with respect to the operators $a^\dagger a$, $-i\partial/\partial x$, $-i\partial/\partial z$, and σ_z . The commutation relations (2a) and (2b) are written in terms of a and a^\dagger as

$$[a, a^\dagger] = 1, \quad [a, a] = [a^\dagger, a^\dagger] = 0. \quad (5)$$

One of the extra terms resulting from the presence of spin-orbit interaction is $-\sqrt{2}C\kappa(a\sigma_+ + a^\dagger\sigma_-)$. This term represents a dynamic interaction between the cyclotron motion and the spin states, and it changes the Landau quantum number and spin states simultaneously, keeping $\{a, a^\dagger\} + \frac{1}{2}\sigma_z$ constant. Another term $C(m_1/\hbar) \times (cE/H)\sigma_y$, which is equivalent to a static external magnetic field directed along the y axis, arises from the influence of classical drift motion along the x axis upon spin states. This effective magnetic field acts only upon the spin which undergoes a rotation of its own axis. The resulting change of the spin states induces the alteration of cyclotron motion via the dynamic interaction. This is the effect which is characteristic of the spin-orbit term in crossed electric and magnetic fields. The electric-field-dependent scalar terms are contributions from the kinetic energy of the transverse drift motion and the electrostatic potential at the position of the oscillation center on the y axis. The last three diagonal terms of \mathcal{H} give rise to only a level shift as a whole and do not change intraband transitions. Since we consider only intraband transitions in this paper, we shall not treat these terms explicitly. In order to see the relative magnitude of the various terms in the Hamiltonian (4), it is convenient to express the energy scale in the unit of the cyclotron energy $\hbar\omega_c$. Thus, let us define the reduced Hamiltonian

$$K = \{\mathcal{H} - (\text{irrelevant diagonal scalar terms})\} / \hbar\omega_c,$$

which is explicitly written as follows:

$$K = \{a, a^\dagger\} + \mu\sigma_z + \lambda\sigma_y - \xi(a\sigma_+ + a^\dagger\sigma_-), \quad (6)$$

where $\mu = \frac{1}{2}g_{11}m_1/m$, $\lambda = CeE/(\hbar\omega_c)^2$, $\xi^2 = \Delta/\hbar\omega_c$, and

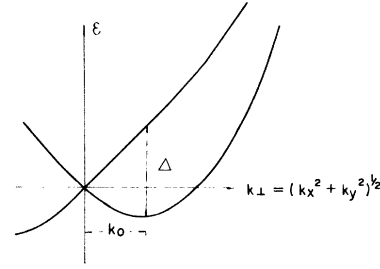


FIG. 1. The energy spectrum of the Γ_7 band as a function of $k_1 = (k_x^2 + k_y^2)^{1/2}$. The radius of the extremum loop k_0 and the spin-orbit splitting at the loop Δ are important parameters characterizing the Γ_7 band.

$\Delta = 2m_1 C^2 / \hbar^2$, which is the spin-orbit splitting between the states on the extremum loop and their spin-conjugate states (see Fig. 1).

We now have three parameters μ , λ , and ξ characterizing the reduced Hamiltonian (6); μ is a constant proportional to g_{11} and m_1 ; ξ is a coupling parameter describing the interaction between the cyclotron motion and the spin state; λ is the effective magnetic field, directed along the y axis and acting only upon the spin. It is also proportional to the transverse electric field. In dealing with the reduced Hamiltonian (6), we shall hereafter abbreviate the basis state $|nk_x k_z \pm\rangle$ for the full Hamiltonian as $|n\pm\rangle$ for the reduced Hamiltonian.

III. SOLUTION FOR THE REDUCED HAMILTONIAN

In order to solve for the reduced Hamiltonian K , we shall consider the following four cases:

- (A) $\lambda \ll \mu$, $\xi \ll 1$, (B) $\lambda \ll \mu$, $\xi \gtrsim 1$,
 (C) $\lambda \gtrsim \mu$, $\xi \ll 1$, (D) $\lambda \gtrsim \mu$, $\xi \gtrsim 1$.

1. Case (A): Weak Electric Field and Weak Coupling, and Case (B): Weak Electric Field and Strong Coupling

When $\lambda = 0$, we can solve the reduced Hamiltonian K exactly¹⁵ by decoupling the secular determinant into the subspace spanned by the states $|n-1, +\rangle$ and $|n, -\rangle$ by making use of the conservation of $\{a, a^\dagger\} + \frac{1}{2}\sigma_z$, which commutes with K . Thus, we obtain the eigenvalues

$$\epsilon_n^{(\mp)} = n \mp \left[\left(\frac{1}{2} - \mu \right)^2 + n \xi^2 \right]^{1/2} \quad (\text{sign } + \text{ only for } n=0) \quad (7)$$

and eigenvectors

$$|n(\mp)\rangle = \begin{Bmatrix} c_n \\ -s_n \end{Bmatrix} |n-1, +\rangle + \begin{Bmatrix} s_n \\ c_n \end{Bmatrix} |n, -\rangle, \quad (8)$$

¹⁵ É. I. Rashba, Usp. Phys. Nauk **81**, 557 (1964) [English transl.: Soviet Phys.—Usp. **7**, 823 (1965)]; É. I. Rashba, Fiz. Tverd. Tela **2**, 1224 (1960) [English transl.: Soviet Phys.—Solid State **2**, 1109 (1960)].

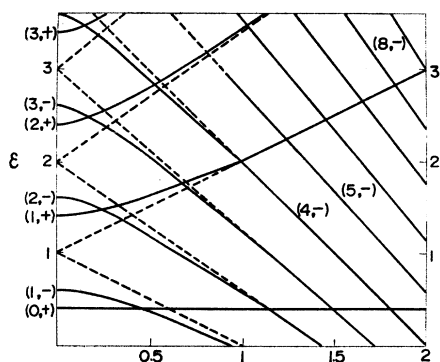


FIG. 2. The energy spectrum of the unperturbed states for the cases (A) and (B) as a function of the "coupling" parameter ξ , where the spin-splitting parameter μ is taken to be 0.1. At the values of $\xi = n + n' \pm 2[nn' + (\frac{1}{2} - \mu)^2]^{1/2}$ ($n > n'$), one encounters an accidental degeneracy between the states $|n(-)\rangle$ and $|n'(\pm)\rangle$. The energy scale is given in units of $\hbar\omega_c$.

where $n = \{a, a^\dagger\} + \frac{1}{2}\sigma_z$, $c_n = \cos(\frac{1}{2}\varphi_n)$, $s_n = \sin(\frac{1}{2}\varphi_n)$, and $\tan \varphi_n = n^{1/2}\xi / (\frac{1}{2} - \mu)$.

The energy eigenvalue $\epsilon_n^{(\pm)}$ of Eq. (7) is plotted in Fig. 2 as a function of ξ . The effect of the spin-orbit term on the energy eigenvalue becomes appreciable when ξ approaches and exceeds unity. In this case, we can observe the spin-orbit effect by resonance experiments. Usually, they are carried out by scanning the external magnetic field at fixed microwave frequencies. Since ξ contains the unknown parameters Δ and m_\perp , it is convenient in practice to plot the resonance spectra as a function of H rather than as a function of ξ . Assuming a resonance peak to be due to a certain transition, we fit the corresponding energy expression to the observed resonance energy by making use of the formula

$$E_n^{(\pm)} \equiv \hbar\omega_c \epsilon_n^{(\pm)} = nA \pm (BH^2 + nDH)^{1/2},$$

where A , B , and D are adjustable constants to be fitted experimentally. The correct assignment for the spectral lines can be attained by confirming whether all the lines observed can be fitted consistently. Thus, we obtain the values of A , B , and D and, hence, those of m_\perp , g_\perp , and C , from the experiment.

The method described here for determining the value of C can be applied only to the case of a quantum limit $\beta = \hbar\omega_c/k_B T \gg 1$. In a high-temperature limit $\beta \ll 1$, we need a discussion of line shape, which will be given in Sec. IV.

As will be discussed later, the spin-orbit splitting Δ for the actual II-VI compounds is not large enough to satisfy the relation $\xi^2 = \Delta/\hbar\omega_c \approx 1$ for the cyclotron frequency $\omega_c \gg 1/\tau$, where τ is a carrier relaxation time. Therefore, we have to carry out the experiment under the condition of $\xi \ll 1$, except possibly for CdSe. In order to investigate the spin-orbit effect in this case, the transverse electric field must be strong enough for λ to approach or exceed μ . This case is treated in case (C).

Before proceeding to the cases of the strong electric field, (C) and (D), the effects of the weak electric field

will be briefly discussed. There is a small correction in energy owing to the presence of the term $\lambda\sigma_y$. If necessary, it can be calculated by second-order perturbation theory. The effect of the weak electric field on the transition probabilities will be treated later. At the values of ξ where the relation

$$\xi^2 = n + n' \pm 2[nn' + (\frac{1}{2} - \mu)^2]^{1/2} \quad (n > n')$$

is satisfied, we find that the states $|n(-)\rangle$ and $|n'(\pm)\rangle$ are accidentally degenerate, as shown in Fig. 2. Degenerate perturbation¹⁶ theory gives splittings of order $\lambda^{n-n'}$ between these states. Apparently, they are quite small for the weak electric field.

2. Case (C): Weak Coupling and Strong Electric Field

Now we shall proceed to the most important case which is realized in the actual II-VI compounds.¹² Since the off-diagonal matrix elements of $\lambda\sigma_y$ in Eq. (6) are arbitrarily large in value, they must be transformed into diagonal parts as follows:

$$\begin{aligned} \tilde{K} &= e^{-i\varphi\sigma_z} K e^{i\varphi\sigma_z} \\ &= \{a, a^\dagger\} + (\mu^2 + \lambda^2)^{1/2} \sigma_z - \xi \Lambda, \end{aligned} \quad (9)$$

where

$$\begin{aligned} \Lambda &= \sigma_+ [(1+c)a + (1-c)a^\dagger] \\ &+ \sigma_- [(1-c)a + (1+c)a^\dagger] + is\sigma_z(a - a^\dagger) \end{aligned} \quad (10)$$

and $\tan \varphi = \lambda/\mu$, $|\varphi| < \frac{1}{2}\pi$, $c = \cos \varphi$, and $s = \sin \varphi$.

We shall for a moment discuss the diagonal part of \tilde{K} . For the state having the Landau quantum number n and the spin quantum number ± 1 with respect to the new σ_z axis, we have the expression for the energy

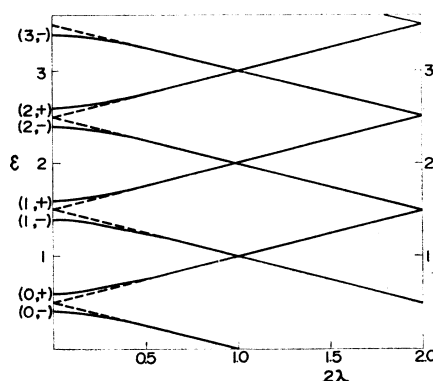


FIG. 3. The energy spectrum of the unperturbed states of the case (C) as a function of the electric-field-dependent effective "magnetic field" 2λ . The spin-splitting parameter μ is taken to be 0.1. At the point 2λ , where $(\mu^2 + \lambda^2)^{1/2} \approx \frac{1}{2}m$ (m is a positive integer) is satisfied, the accidental degeneracy between the states $|n-m(+)\rangle$ and $|n(-)\rangle$ occurs. The energy scale is given in units of $\hbar\omega_c$.

¹⁶ For example, L. D. Landau and E. Lifshitz, *Quantum Mechanics: Non-Relativistic Theory* (Addison-Wesley Publishing Co., Inc., Reading, Massachusetts, 1958).

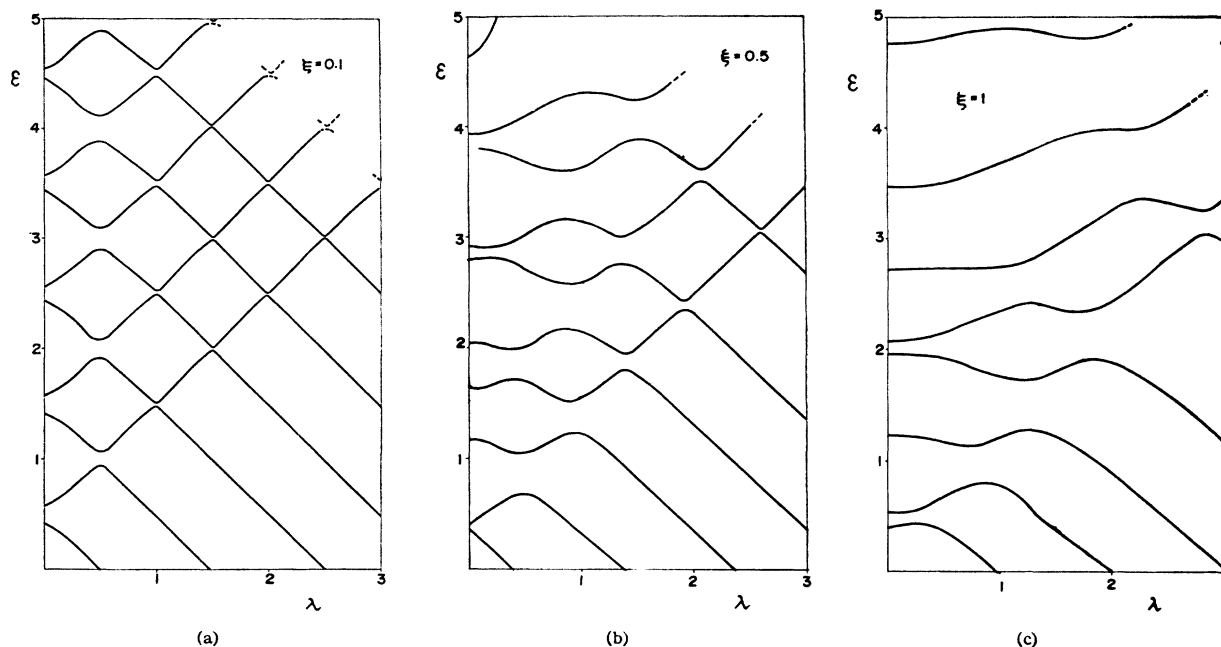


FIG. 4. Computer generated ϵ - λ curves. The numerical solution was obtained by diagonalizing a 12×12 matrix in the $|n, \pm\rangle$ basis. (a) $\mu = \xi = 0.1$. This corresponds to the case (C) (see Fig. 3). (b) $\mu = 0.1$, $\xi = 0.5$. (c) $\mu = 0.1$, $\xi = 1$. As ξ and λ increase, energy levels become strongly repulsive. As λ increases for a given ξ , the energies of higher-lying levels begin to increase monotonically. At this point, the variational solution loses its validity. This can also be seen by examining how the amplitudes of the variational solutions are distributed over the basis states $|n, \pm\rangle$. Dashed lines show these points.

eigenvalue

$$\epsilon_n(\pm) + n + \frac{1}{2} \pm (\mu^2 + \lambda^2)^{1/2}. \quad (11)$$

This is plotted as a function of 2λ in Fig. 3. As λ approaches μ with increasing electric field, the spin splitting $2(\mu^2 + \lambda^2)^{1/2}$ develops an appreciable electric field dependence. In an extremely strong electric field, where $\lambda \gg \mu$ is satisfied, this spin splitting tends to have a linear dependence upon the electric field, being asymptotically equal to 2λ ; and the spin axis approaches the direction of the electric field as $\varphi \rightarrow \frac{1}{2}\pi$. This can simply be seen from the expression of the reduced Hamiltonian K of Eq. (6). If we neglect μ as compared to λ in K , the effective "magnetic" field acting upon the spin is directed along the y axis, and consequently the spin splitting becomes 2λ .

From the measured value of ω_c and the λ dependence of the spin splitting, we obtain the value of C as well as the other band-mass parameters. Actually, the following prescriptions apply:

(1) The condition for the "spin resonance" at the microwave frequency ω is

$$\omega/\omega_c = 2(\mu^2 + \lambda^2)^{1/2},$$

which can be rewritten as

$$(2E)^2 = (\omega/c k_0)^2 H^2 - (g_{11}\beta/c k_0)^2 H^4, \quad (12)$$

where $k_0 = m_1 C/\hbar^2$. In the experimental situation where the microwave frequency is fixed, Eq. (12) prescribes

the functional relation between $(2E)^2$ and H^2 . Therefore, fitting the equation to the experimentally derived $(2E)^2$ versus H^2 curve, we obtain the values of k_0 and g_{11} .

(2) The observed value of the cyclotron frequency ω_c gives the effective mass m_1 , which in turn determines the value of C from k_0 .

When $\xi \ll 1$, the perturbation $-\xi\Lambda$ is small enough to be neglected. If necessary, the energy correction due to $-\xi\Lambda$ can be treated by second-order perturbation theory. At the value of 2λ where $2(\mu^2 + \lambda^2) \approx m$ is satisfied, we find an accidental degeneracy between the states $|n-m, (+)\rangle$ and $|n, (-)\rangle$. Then, m th order degenerate perturbation theory¹⁶ gives a very small splitting of order ξ^m and a mixing of the states.

3. Case (D): Strong Coupling and Strong Electric Field

As we have already noted, it is impossible for the actual II-VI compounds to fulfill the condition $\xi \gg 1$ for cyclotron frequencies $\omega_c > 1/\tau$. However, for completeness and as a supplement to the lower-order perturbation theory described so far, we shall give a variational solution for K which is valid for this case as well as for the previous cases.

In the case (D), every term in K gives a contribution of nearly the same order of magnitude. Therefore, we have to solve a secular equation numerically using the basis consisting of the Landau and spin states $|n\pm\rangle$ by truncating this secular equation into a finite-rank de-

terminant. (It may be expected that the convergence of the variational solution whose basis vectors are a finite set of Landau and spin states is not sufficiently good when $\xi \rightarrow \infty$ and $\lambda \rightarrow \infty$. In that case, however, our one-band formalism loses its validity, and we do not consider such a case.) The detailed procedure for the numerical solution is given in the Appendix.

A numerical calculation has been carried out by diagonalizing a 12×12 submatrix in Eq. (A4) for the following three cases: (a) $\mu = 0.1$, $\xi = 0.1$, $\lambda = 0 \sim 3$; (b) $\mu = 0.1$, $\xi = 0.5$, $\lambda = 0 \sim 3$; (3) $\mu = 0.1$, $\xi = 1$, $\lambda = 0 \sim 3$. To compare the numerical solutions presented here with the analytical solutions obtained previously, we have included cases (A), (B), and (C) for the numerical calculations. The case (a) corresponds to cases (A) and (C); both cases (b) and (c), to cases (B) and (D). The results are illustrated in Figs. 4(a), 4(b), and 4(c), respectively. The ϵ - λ relation in Fig. 4(a) is exactly what we expected in case (C). That the convergence of the variational solutions is satisfactory is confirmed by examining how the amplitudes of the eigenvectors are distributed over the basis functions. As ξ and λ increase, the mixing of the basis states $|n\pm\rangle$ increases, so that the energy levels become strongly repulsive. It is characteristics of all of Figs. 4(a), 4(b), and 4(c) that, as λ increases, the lower-lying levels decrease together, keeping the separations between adjacent levels nearly constant. The origin of this phenomenon can be understood by consulting the analytical solution of Eq. (11) for case (C). Since the energy eigenvalues have a strong electric field dependence, we can determine the value of C as well as the other band-mass parameters experimentally on the basis of this solution.

IV. SELECTION RULES AND LINE SHAPE OF INTRABAND TRANSITIONS

We now proceed to discuss the selection rules and line shapes for intraband transitions. General expressions for the imaginary parts of the frequency-dependent dielectric constant and magnetic susceptibility for left- and right-circularly polarized fields are given by¹⁵

$$\epsilon''(\omega) = \frac{\pi e^2}{\hbar \Omega \omega^2} \int_{-\infty}^{\infty} dt e^{i\omega t} \langle [v_{\mp}(t), v_{\pm}] \rangle \quad (13)$$

and by

$$\mu''(\omega) = \frac{\pi g^2 \beta_0^2}{\hbar \Omega} \int_{-\infty}^{\infty} dt e^{i\omega t} \langle [\sigma_{\mp}(t), \sigma_{\pm}] \rangle, \quad (14)$$

respectively. Here, $v_{\pm} = v_x \pm i v_y$; $\sigma_{\pm} = \frac{1}{2}(\sigma_x \pm i \sigma_y)$; $v_{\mp}(t)$ and $\sigma_{\mp}(t)$ are the Heisenberg operators for v_{\mp} and σ_{\mp} at time t ; the angular bracket denotes the thermal average; Ω is the total volume of the system; g is an appropriate g factor; and β_0 is the Bohr magneton. The velocity operators for our Hamiltonian are obtained as

$$v_x = \frac{\partial H}{\partial p_x} = \frac{cE}{H} + \frac{1}{\sqrt{2}} \frac{\hbar \kappa}{m_1} \left(\frac{a - a^\dagger}{i} + \xi \sigma_y \right), \quad (15a)$$

$$v_y = \frac{\partial H}{\partial p_y} = \frac{1}{\sqrt{2}} \frac{\hbar \kappa}{m_1} (a + a^\dagger - \xi \sigma_x), \quad (15b)$$

$$v_{\pm} = \pm i \frac{\sqrt{2} \hbar \kappa}{m_1} \begin{cases} a^\dagger + \xi \sigma_- \\ a + \xi \sigma_+ \end{cases}. \quad (15c)$$

In the Γ_7 band, there are various intraband electric dipole transitions combining spin flip with multiple quantum transitions. It should be emphasized that these additional intraband transitions in crossed fields are entirely due to the effects of the spin-orbit coupling term. In a simple band in crossed fields, the only allowed electric dipole transition is the one with $\Delta n = \pm 1$ and $\Delta s = 0$. Multiple quantum transitions due to the transverse drift motion are forbidden in the intraband case for a band with quadratic dispersion.

First, we shall discuss the limiting cases (A), (B), and (C), where the perturbative expansions have sufficient convergence. The matrix elements of the velocity operators between the true eigenstates can be expressed as a linear combination of the matrix elements between the unperturbed states by expanding the true eigenstates in terms of the unperturbed states through perturbation theory. We consider only the lowest-order nonzero matrix elements between the given true eigenstates, because we have assumed rapid convergence of the perturbative expansions.

1. Case (A)

With the aid of Eqs. (8) and (15c), and by the method described above, the following transition probabilities are obtained for cyclotron resonance:

$$|(n+1(+)) \langle v_+ | n(+) \rangle|^2 = v_0^2 [(n+1)^{1/2} c_n c_{n+1} + n^{1/2} s_n s_{n+1}]^2, \quad (16a)$$

$$(1 - \zeta_n^{(-)}),$$

$$|(n+1(-)) \langle v_+ | n(-) \rangle|^2 = v_0^2 [n^{1/2} c_n c_{n+1} + (n+1)^{1/2} s_n s_{n+1}]^2, \quad (16b)$$

$$(1 - \zeta_n^{(-)});$$

and for combination resonance:

$$|(n+1(-)) \langle v_+ | n(+) \rangle|^2 = v_0^2 [(n+1)^{1/2} c_n s_{n+1} - n^{1/2} s_n c_{n+1}]^2, \quad (17a)$$

$$(1 - \zeta_n^{(+)}),$$

$$|(n+1(-)) \langle v_- | n(+) \rangle|^2 = (\xi v_0)^2 (c_n c_{n+1})^2, \quad (17b)$$

$$(1 - \zeta_n^{(+)}),$$

$$|(n+1(-)) \langle \sigma_+ | n(+) \rangle|^2 = (c_n c_{n+1})^2, \quad (18)$$

$$(1 - \zeta_n^{(+)}).$$

Here, $|n(\pm)\rangle$ stands for the true eigenstate corresponding to the unperturbed state $|n(\pm)\rangle$, and $v_0 = \sqrt{2} \hbar \kappa / m_1$. The energy difference between the initial and final states for each transition is shown in the parentheses, where

$$\xi_n^{(\pm)} = \left[\left(\frac{1}{2} - \mu \right)^2 + (n+1) \xi^2 \right]^{1/2} \pm \left[\left(\frac{1}{2} - \mu \right)^2 + n \xi^2 \right]^{1/2}.$$

The intensity of the combination resonance (17) is weaker than that of the cyclotron resonance by a factor of order ξ^2 . This combination resonance occurs also in the case of $\lambda=0$ and has been treated extensively by Rashba.¹⁵ The combination resonance (18) is due to a magnetic dipole transition, which may more appropriately be called a spin resonance in the usual terminology. This difference arises from the definition of the state (8), and the transition (18) will be hereafter called a combination resonance, according to our definition.

Thus far, we have considered only the electric dipole transitions having intensities independent of λ . Because of the presence of $\lambda\sigma_y$, there occur other types of transitions having intensities of order $(\lambda\xi^2)^2$ or $(\lambda\xi^3)^2$, etc., relative to the intensity of the cyclotron resonance. In the case of $\xi\ll 1$, however, these higher-order transitions cannot be observed because of their small transition probabilities. This is actually the case for most II-VI compounds. It follows that actually, in these crystals, no transitions can be seen other than those observed in the case of $\lambda=0$, until λ becomes comparable to or greater than μ .

There are also magnetic dipole transitions other than (18) whose intensities are of order ξ^2 or higher, relative to that of the transition (18).

In the quantum limit $\beta = \hbar\omega_c/k_B T \gtrsim 1$, each resonance line corresponds to a single transition between low-lying quantum states (not considering the degeneracies with respect to k_x and k_z). Therefore, the discussion given so far is adequate for identifying resonance lines. The condition for the quantum limit is not always satisfied for cyclotron resonance and combination resonance, however. In a high-temperature limit $\beta\ll 1$, each resonance peak consists of many overlapping lines, each of which corresponds to a specific transition whose initial states are thermally distributed over states having large values of n . In order to analyze the resonance spectra, we need the envelope function for these overlapping lines. To obtain them, instead of evaluating Eq. (13) rigorously, we calculate the following quantity:

$$I(\omega) = \sum_{1=(nk_x k_z \pm)} M_{21}(f_1 - f_2)\delta(\omega + \epsilon_1 - \epsilon_2), \quad (19)$$

where M_{21} is the square of the matrix element for the transition $1 \rightarrow 2$; ϵ_1 and ϵ_2 are the energies of the states 1 and 2 (in units of $\hbar\omega_c$); and ω is the frequency for an external field, measured in units of the frequency ω_c . Boltzmann statistics are used for electron distribution functions f_1 and f_2 , which are defined such that $f_i = e^{-\beta\epsilon_i}/\sum_1 e^{-\beta\epsilon_1}$ ($i=1, 2$). Since $\epsilon_2 - \epsilon_1$ and M_{21} are independent of k_x and k_z , Eq. (19) may be simplified to

$$I(\omega) = \frac{1 - e^{-\beta\omega}}{Z} \sum_{n\pm} M_{21} e^{-\beta\epsilon_n} \delta^\pm(\omega - \omega_n^\pm), \quad (20)$$

where ϵ_n^\pm is the part of ϵ_1 which depends only on n and

spin states;

$$Z = \sum_{n\pm} e^{-\beta\epsilon_n^\pm}; \quad \omega_n^\pm = \epsilon_2 - \epsilon_1.$$

Solving the equation

$$\omega_n^\pm = \omega \quad (21)$$

with respect to n , we obtain n in terms of ω . Substituting this into Eq. (21), we have the expression for $I(\omega)$ in the following form:

$$I(\omega) = \frac{1 - e^{-\beta\omega}}{Z} \sum_{\pm} F^\pm(\omega) \sum_n \delta(\omega - \omega_n^\pm), \quad (22)$$

where

$$F^\pm(\omega) = M_{21} e^{-\beta\epsilon_n^\pm} \Big|_{\omega_n^\pm = \omega}. \quad (23)$$

Replacing the sum over n by an integral over n ,

$$\begin{aligned} D^\pm(\omega) &= \sum_n \delta(\omega - \omega_n^\pm) \\ &\simeq \int_0^\infty dn \delta(\omega - \omega_n^\pm) \\ &= \left| \frac{\partial n}{\partial \omega} \right|_{\omega_n^\pm = \omega}, \end{aligned} \quad (24)$$

and substituting Eqs. (23) and (24) into Eq. (22), we obtain

$$I(\omega) = [(1 - e^{-\beta\omega})/Z]G(\omega), \quad (25)$$

where

$$\begin{aligned} G(\omega) &= \sum_{\pm} G^\pm(\omega) \\ &= \sum_{\pm} F^\pm(\omega) D^\pm(\omega). \end{aligned} \quad (26)$$

We now apply the result to cyclotron and combination resonances. Even for large values of n , the experiment of cyclotron resonance for CdS indicates that $\varphi_n \ll 1$. It follows that $s_n \approx \frac{1}{2}$, $\tan \varphi_n \sim n^{1/2} \xi$, and $c_n \approx 1$. Hence, we have $M_{21} \approx n v_0^2$ for cyclotron resonance. Following the procedure described above and making use of the relation

$$\omega_n^\pm = 1 \pm \xi_n^{(-)}, \quad (27)$$

we obtain the expression for $G^\pm(\omega)$ for cyclotron resonance as follows:

$$\begin{aligned} G^\pm(\omega) &= F(\omega) D(\omega), \quad \omega \gtrsim 1 \\ &= 0, \quad \omega \lesssim 1 \end{aligned} \quad (28)$$

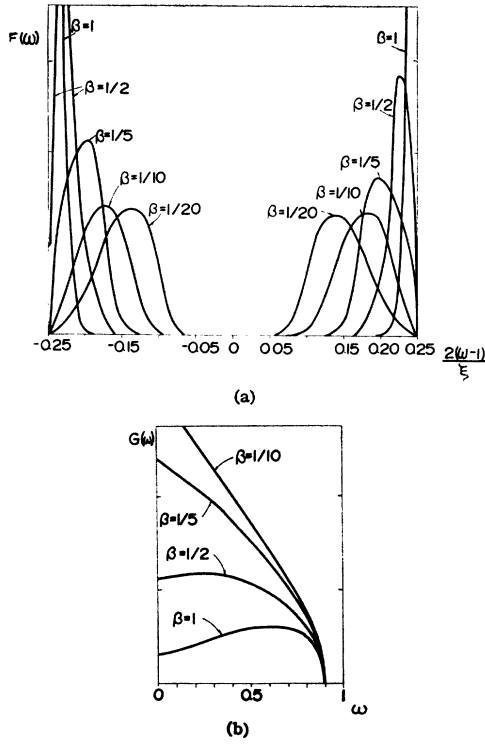


FIG. 5. The line shape of cyclotron and combination resonance for case (A) in the high-temperature limit $\beta = \hbar\omega_c/k_B T \ll 1$. (a) Cyclotron resonance. The function $F(\omega)$ of Eq. (29) is plotted for $\xi = \mu = 0.1$. As temperature increases (β decreases), the two peaks are broadened and move toward each other. The curves are normalized so that the total area below the curve is identical. (b) Combination resonance $G(\omega)$ as given by Eqs. (32), (34), and (35) is plotted for $\xi = \mu = 0.1$. A broad peak can be seen for the cases $\beta = \frac{1}{2}$ and $\beta = 1$.

where

$$F(\omega) = v_0^2 \left[\frac{1}{4} \left(\frac{\xi}{\omega-1} - \frac{\omega-1}{\xi} \right)^2 - \left(\frac{\frac{1}{2} - \mu}{\xi} \right)^2 \right] \times \exp \left[-\frac{\beta}{4} \left(\frac{\xi}{\omega-1} - \frac{\omega-1}{\xi} + \xi \right)^2 \right], \quad (29)$$

$$D(\omega) = \frac{1}{2\xi^2} \left| (\omega-1) \left(1 - \frac{\xi^4}{(\omega-1)^4} \right) \right|. \quad (30)$$

In Eq. (29), we have omitted a constant factor

$$\exp \left\{ \beta \left[\left(\frac{1}{2} - \mu \right)^2 / \xi^2 + \frac{1}{4} \xi^2 \right] \right\}.$$

The functions $F(\omega)$ and $D(\omega)$ are defined in the region

$$|\omega-1| < \xi^2 \left[\left(\frac{1}{2} - \mu \right)^2 + \left\{ \left(\frac{1}{2} - \mu \right)^2 + \xi^2 \right\}^{1/2} \right]^{-1}. \quad (31)$$

Combining Eqs. (29) and (30) with Eq. (28), we obtain

$$G(\omega) = F(\omega)D(\omega), \quad (32)$$

which is defined in the region (31).

The transition matrix elements for combination resonance is given by $M_{21} \approx (v_0 \xi)^2$ for (17) and by $M_{21} \approx 1$

for Eq. (18). The transition energy is

$$\omega_n = 1 - \zeta_n^{(+)}. \quad (33)$$

Hence, we have

$$F(\omega) = M_{21} \exp \left[-\frac{\beta}{4} \left(\frac{1-\omega}{\xi} - \frac{\xi}{1-\omega} + \xi \right)^2 \right], \quad (34)$$

$$D(\omega) = \frac{1}{2\xi^2} \left| (1-\omega) \left(1 - \frac{\xi^4}{(1-\omega)^4} \right) \right|, \quad (35)$$

and $G(\omega)$ is given by Eqs. (32), (34), and (35). The same factor as was omitted in Eq. (29) was also omitted in Eq. (34). Functions $F(\omega)$ of Eq. (34) and $D(\omega)$ of Eq. (35) are defined in the region

$$0 < \omega < \frac{1}{2} + \mu - \left[\left(\frac{1}{2} - \mu \right)^2 + \xi^2 \right]^{1/2}. \quad (36)$$

The function $F(\omega)$ of Eq. (29) is illustrated in Fig. 5(a). From Eq. (27), it may be found that the left and right peaks correspond to the transitions between states with $-$ and $+$ spin, respectively. At low temperatures, the location of the sharp peaks are near $\omega \approx 1 - \xi^2/(1-2\mu)$ and $\omega \approx 1 + \xi^2/(1-2\mu)$, respectively. As the temperature increases (or β decreases), transitions between higher-lying levels become dominant. The two peaks which were split at low temperatures are broadened and come close to each other. The function $G(\omega)$ given by Eqs. (32), (34), and (35) is shown in Fig. 5(b). This has a broad peak at low temperatures. At higher temperatures, $G(\omega)$ is a monotonically decreasing function and vanishes at $\omega = 1 - \xi$.

2. Case (B)

The transition probabilities of Eqs. (16) and (17) are, in this case, of the same order. Other transitions with the relative intensities of $(\lambda \xi^2)^2$ or $(\lambda \xi^3)^2$ also become important, so that we need the expression for the transition probabilities of these higher-order processes. Since there are many intermediate states connecting initial states with final ones, they have quite complicated expressions. Magnetic dipole transitions other than (18) (with relative intensities of ξ^2 , etc.) also have intensities of the same order as that of the transition (18). As the case (B) has no practical importance, the expressions for these transition probabilities will not be given here.

In the high-temperature limit $\beta \ll 1$, the function $G(\omega)$ is calculated only for cyclotron resonance and for combination resonance. Since $\varphi_n \gg 1$ for large values of n , we have $\varphi_n \approx \frac{1}{2}\pi$ and $s_n \approx c_n \approx 1/\sqrt{2}$, and hence $M_{21} \approx v_0^2 n$ for the cyclotron resonance (16). The expression for $G(\omega)$ is the same as Eq. (31). In the case of $\xi > 1$, however, $\omega_n^{(-)}$ of Eq. (27) is negative for $n < (1/4)(\xi - 1/\xi)^2 - (1/2 - \mu)^2/\xi^2$. In this case, the initial and final states of the transition are inverted, so that the corresponding expression for $G(\omega)$ takes a different form. This transition can be observed for a limited range of n , and hence in the quantum limit, if ξ is not too large.

Since $M_{21} \approx (v_0/4)^2/n$ for combination resonance (17), we obtain

$$F(\omega) = \frac{v_0}{4} \exp \left[-\frac{\beta(1+\omega)}{4} \left(\frac{\xi}{1+\omega} + \frac{\xi}{1+\omega} - \xi \right)^2 \right] / \frac{1}{4} \left(\frac{\xi}{1+\omega} - \frac{1+\omega}{\xi} \right)^2 - \left(\frac{\frac{1}{2} - \mu}{\xi} \right)^2 \quad (37)$$

and

$$D(\omega) = \frac{1+\omega}{2\xi^2} \left| 1 - \frac{\xi^4}{(1+\omega)^4} \right|. \quad (38)$$

From Eq. (18), the transition probability for combination resonance due to magnetic dipole transitions is approximately given by $M_{21} \approx \frac{1}{2}$, and hence we have

$$F(\omega) = \frac{1}{2} \exp \left[-\frac{\beta(1+\omega)}{4} \left(\frac{\xi}{1+\omega} + \frac{\xi}{1+\omega} - \xi \right)^2 \right]. \quad (39)$$

The function $D(\omega)$ is given by Eq. (38).

3. Case (C)

Since this case is of special importance for the actual II-VI compounds, the transition probabilities will be discussed in relative detail. With a similar procedure to that followed in the case (A), they are obtained for cyclotron resonance as

$$|(n \pm 1, (\pm)) |v_+ |n, (\pm))|^2 = v_0^2(n+1), \quad (40)$$

(1),

and for spin resonance as

$$|(n, (+)) |v_+ |n, (-))|^2 = \left[v_0(1-c) \left(1 - \frac{n+1}{1-\bar{g}} \right) \right]^2, \quad (41a)$$

(\bar{g}),

$$|(n, (+)) |v_- |n, (-))|^2 = \left[v_0(1-c) \left(1 - \frac{n}{1-\bar{g}} \right) \right]^2, \quad (41b)$$

(\bar{g}),

$$|(n, (+)) |\sigma_x |n, (-))|^2 = 1, \quad (42)$$

(\bar{g}),

where $|n(\pm))$ stands for the true eigenstate corresponding to the unperturbed one $|n(\pm))$ of Eq. (11), and the energy difference $\bar{g} = 2(\mu^2 + \lambda^2)^{1/2}$. The intensities of the spin resonances (41) are of order ξ^2 relative to that of the cyclotron resonance. Electric dipole transitions other than (40) and (41) are all higher order in ξ and cannot be observed for the actual crystals. Spin resonance (42) is due to a magnetic dipole transition that is due to the oscillating magnetic fields with their polarization directed along the x axis.

TABLE I. Transition probabilities due to v_+ between the lowest three levels, designated as 1, 2, and 3, starting from the bottom, for the cases (a) $\mu = \lambda = 0.1$, $\xi = 1$ and (b) $\lambda = 0.1$, $\xi = \lambda = 1$.

v_+	1 → 2	1 → 3	2 → 1	2 → 3	3 → 1	3 → 2
a	0.813	1.21	0.332	0.0367	0.191	0.0361
b	1.23	0.0906	0.0262	0.0520	0.123	0.122

The results described here for the transition probabilities are essentially the same as those for case (A) in the following sense: The only electric dipole transition having intensity independent of the magnitude of ξ is cyclotron resonance. The additional transitions due to the presence of the spin-orbit term have intensities of order ξ^2 or higher relative to that of the cyclotron resonance, even if a strong electric field is applied. It is in the case of $\xi \approx 1$ that these additional transitions become comparable to the cyclotron resonance. This can be seen directly from the Hamiltonian (6). The term $\lambda \sigma_y$ turns the direction of the spin axis to modify the spin part of the wave function, but not the orbital part directly. The mixing of the states $|n, \pm\rangle$ and $|n \pm 1, \pm\rangle$ arises only through the term containing ξ . Incidentally, if the direction of the magnetic field is rotated in the y - z plane without the electric field, mixings of the states $|n, \pm\rangle$ occur in a similar manner, causing additional transitions with intensities of order ξ^2 relative to that of the cyclotron resonance. In this sense, the effect of the transverse electric field on the transition probabilities is, roughly speaking, the same as that of rotating the external magnetic field in a plane including the c axis.

4. Case (D)

The qualitative features of the transition probabilities will be briefly given. Now, since n and σ_z are not good quantum numbers, the eigenstates of K cannot be specified by these quantum numbers. The transition matrix elements are determined by the variational wave functions with their amplitude distributed over many Landau and spin states $|n \pm\rangle$, so that every transition is allowed without any simplifying selection rule. For the same reason, the words "cyclotron resonance," "spin resonance," etc., lose their rigorous physical meaning.

Transition probabilities between low-lying levels may be calculated from the numerical solutions obtained in Sec. II. The results of the calculation are given for electric dipole transitions for cases (a) $\xi = 1$, $\mu = \lambda = 0.1$; (b) $\mu = 0.1$, $\xi = \lambda = 1$. The lowest three levels are designated as 1, 2, and 3. The transition probabilities between these levels are given in Table I.

V. DISCUSSION

To begin with, we wish to make an estimate of the order of magnitude of C . The application of the $\mathbf{k}\cdot\mathbf{P}$ perturbation theory to the quasicubic model,¹³ which is appropriate for the most II-VI compounds, yields the following expressions for the band slope C of the Γ_7

TABLE II. Band-mass parameters of wurtzite-type II-VI compounds. E_A , E_B , and E_C are the energy separation between the Γ_7 conduction band and the Γ_9 (A) valence band, the separation between the Γ_7 conduction band and the Γ_7 (B) valence band, and the separation between the Γ_7 conduction band and the Γ_7 (C) valence band, respectively. Δ_{so} and Δ_{tr} are the spin-orbit splitting and the trigonal-field splitting of the valence bands of the "cubic" crystal at the Γ point. m_e and g_e are the effective mass and g factor of an electron in the Γ_7 conduction band. The value of the linear \mathbf{k} spin-orbit coupling parameter C for CdS is calculated from the experimental value of C for the Γ_7 valence band. The value of C for CdSe is taken from the upper limit Hopfield has placed by the analysis of exciton spectra. The estimated values for C based upon the quasicubic model, are listed for CdS and CdSe (in the parenthesis) and for ZnS. Note that these estimated values may be an order of magnitude larger than the true values. Δ is the spin-orbit splitting at the extremum loop of the Γ_7 -conduction band in \mathbf{k} space, while k_0 is the radius of the loop. The critical magnetic field H_c is defined by the relation $\xi^2=1$, while the critical electric field E_c is defined by the relation $\xi^2=1$ and $\lambda/\mu=1$. The first seven columns are cited from M. Aven and V. S. Prener, *Physics and Chemistry of II-V Compounds* (North-Holland Publishing Co., Amsterdam, 1967).

	E_A (eV)	E_B (eV)	E_C (eV)	Δ_{so}	Δ_{tr}	m_e	g_e	C (eV cm)	Δ (μV)	k_0 (cm^{-1})	H_c (G)	E_c (V/cm)
CdS	2.5831	2.5981	2.661	0.065	0.027	0.205 ± 0.01	$1.78 \pm 0.05(\parallel)$ $1.72 \pm 0.1(\perp)$	0.3×10^{-10} (0.6×10^{-10})	0.47 (1.8)	0.8×10^4 (1.4×10^4)	8 (32)	0.70×10^{-3} (5.6×10^{-3})
CdSe	1.8415	1.8678	2.274	0.42	0.041	0.13 ± 0.03	$0.51 \pm 0.05(\perp)$ $0.6 \pm 0.1(\parallel)$	2×10^{-10} (6.8×10^{-10})	14 (160)	3.2×10^4 (1.2×10^6)	150 (1700)	1.8×10^{-2} (0.70)
ZnS	3.9115	3.9399	4.030	0.092	0.055	0.34 ± 0.02^a	$2.3 \pm 0.1(\perp)$ $2.0(\parallel)$	0.6×10^{-10}	2.7	2.0×10^4	80	2.9×10^{-2}

^a H. Kuimoto, S. Shionoya, T. Koda, and R. Hioki, *J. Phys. Chem. Solids* **29**, 935 (1968).

bands at $\mathbf{k}=0$:

$$\frac{\Delta_{so}U}{3E_\theta^2} i \left\langle \Gamma_{1c} \left| \frac{\hat{p}_x}{m} \right| \Gamma_{4v^x} \right\rangle \quad (\Gamma_7 \text{ conduction band}), \quad (43)$$

$$\frac{2\Delta_{tr}U}{3E_\theta \Delta E_{BC}} i \left\langle \Gamma_{1c} \left| \frac{\hat{p}_x}{m} \right| \Gamma_{4v^x} \right\rangle \quad (\Gamma_7 \text{ valence band}^{17}), \quad (44)$$

where Δ_{so} and Δ_{tr} are the spin-orbit and the trigonal-field splitting of the valence band, respectively. U is the interband matrix element of the trigonal field between $|\Gamma_{1c}\rangle$ and $|\Gamma_{4v^x}\rangle$ states and is approximately given by $(E_\theta \Delta_{tr})^{1/2}$ as long as $E_\theta \ll \Delta_{so}, \Delta_{tr}$. E_θ is the band gap of the "cubic" crystal, and ΔE_{BC} is the energy separation between the $\Gamma_7(B)$ and $\Gamma_7(C)$ bands. The state vectors $|\Gamma_{1c}\rangle$ and $|\Gamma_{4v^x}\rangle$ are the irreducible representations of the cubic group of the conduction and valence band states. The momentum matrix element $\langle \Gamma_{1c} | \hat{p}_x | \Gamma_{4v^x} \rangle$ can be estimated from the electron effective mass to be about 1×10^{-19} (cgs units) for most II-VI compounds.⁹ The calculated values of C , using the momentum matrix element and other relevant band parameters, are listed in Table II. In the case of ZnO, the interpretation of the observed exciton spectra is still controversial and the quasicubic model seems to be insufficient.¹⁸ However, the value of C for the conduction band of ZnO is expected to be smaller than that of other II-IV compounds, because of the small spin-orbit coupling of the atomic oxygen.

The only observed value of C is that of the Γ_7 valence band of CdS, about 0.5×10^{-9} eV cm¹¹, which is an order of magnitude smaller than the calculated value. This result indicates that the calculations based upon the quasicubic model may give an overestimate of the spin-orbit parameter C , as pointed out by Hopfield.⁹ By

¹⁷ H. Hasegawa, *Bussei* **6**, 36 (1965) (circulation in Japanese).

¹⁸ Y. S. Park, C. W. Litton, T. C. Collins, and D. C. Reynolds, *Phys. Rev.* **143**, 572 (1966).

making use of the observed value, a better estimate can be made for CdS. Since the weakness of the estimate described above is in the estimate of U , we eliminate U by Eqs. (43) and (44) to obtain a relation between the C 's for conduction and valence bands:

$$\frac{C_{cb}}{C_{vb}} = \frac{\Delta_{so} \Delta E_{BC}}{\Delta_{tr} E_\theta} = 0.06. \quad (45)$$

Substituting $C_{vb} = 0.5 \times 10^{-9}$ eV cm into Eq. (35), we have $C_{cb} = 0.3 \times 10^{-10}$ eV cm. This value is listed for CdS in Table II. From the analysis of exciton spectra,⁹ Hopfield placed the upper limit on C_{cb} for CdS as 1×10^{-10} and for CdSe as 2×10^{-10} . The value of C_{cb} for CdSe calculated by Eq. (43) is larger than the upper limit which is listed for C_{cb} for CdSe in the table. Values for CdS and CdSe calculated by Eq. (43) are shown in parentheses. Using the values of C in the Table, we obtain those of the spin-orbit splitting Δ , the radius of the extremum loop k_0 , a critical magnetic field H_c (the intensity of the magnetic field at $\xi=1$), and a critical electric field E_c (the intensity of the electric field at $\xi=\lambda/\mu=1$), which are given in Table II. These parameters give a criterion for the frequency of incident photon and for the intensity of crossed electric and magnetic fields experiments necessary for cases (A), (B), (C), or (D) to be carried out.

Considering all the results obtained so far, we discuss the possibility of observing the spin-orbit effects on the Γ_7 conduction band for actual II-VI compounds. In order to detect a sharp resonance line, the cyclotron frequency $\omega_c/2\pi$ must satisfy the condition $\omega_c > 1/\tau$. If we take the cyclotron frequency $\omega_c/2\pi$ from Sawamoto's experiment¹⁹ as 50 GHz and use the value of Δ given in Table II, we find the coupling parameter ξ^2 to be 0.0023 for CdS, 0.068 for CdSe, and 0.013 for ZnS. This means that case (A) or (C) is realized for these crystals in 50

¹⁹ K. Sawamoto, *J. Phys. Soc. Japan* **18**, 1224 (1963).

GHz frequency region. The corresponding magnetic fields $H = H_c/\xi^2$ are 3,600 G for CdS, 2320 G for CdSe, and 6060 G for ZnS. The transverse electric field necessary for realizing case (C) is given by $E = (\lambda/\mu)E_c/\xi^4$. From the values of E_c in Table II, we obtain the value of E to be 130 V/cm for CdS, 3.7 V/cm for CdSe, and 17 V/cm for ZnS, where λ/μ is set equal to unity. Thus, it is found that case (C) is realized under a reasonable electric field intensity.

The coupling parameter ξ^2 for CdS is so small that, in case (A), the two peaks could not be resolved as they can be in Fig. 5(a) for cyclotron resonance. Indeed, the resonance spectra observed by Sawamoto¹⁹ does not seem to present any indication of an extra peak. This is an experimental verification that the importance of the spin-orbit effect relative to cyclotron motion is negligible for CdS in the region of 50 GHz. On the other hand, the value of ξ^2 is sufficiently large for CdSe, so that the peak structure in cyclotron resonance and combination resonance due to electric dipole transitions are expected to be observed. Since the combination resonance (due to electric or magnetic dipole transitions) has a broad peak in the high-temperature limit (see Fig. 5), the experiment of combination resonance must be carried out in the quantum limit.

In case (C), the expression for the energy eigenvalue of Eq. (11) indicates that the spin resonance exhibits a sharp peak. Accordingly, the information necessary to determine the band parameters m_L , g_{11} and C is furnished by the spin resonance, combined with the result of cyclotron resonance. The value of ξ^2 indicates that a spin resonance due to magnetic dipole transitions may be observed for CdS, and one due to electric and magnetic dipole transitions for CdSe.

In case (C), however, the effects of transverse drift motion upon the line shape must be taken into account. Although rigorous discussion requires the evaluation of $\epsilon''(\omega)$ of Eq. (13) and $\mu''(\omega)$ of Eq. (14), a qualitative account may be given without such evaluation. If the transverse drift velocity, given by $v_d = cE/H = (\lambda/\mu) \times (\omega_c/k_0)$, exceeds the velocity of sound in the crystal in the high-frequency region of ω_c , a phonon cloud builds up around the electron,²⁰ so that the relaxation effects quickly destroy the dynamic coherence of the electronic states, resulting in a line broadening. According to the value of k_0 calculated from that of C given in Table II, the drift velocity is, indeed, one or two orders of magnitude larger than the velocity of sound (typically 1.5×10^5 cm/sec) for the intensities of the crossed electric and magnetic fields corresponding to $\xi = \lambda/\mu = 1$ and $\omega_c/2\pi = 50$ GHz. This puts a serious limitation on the resonance experiment. However, the difficulty can be overcome by observing the resonance signal in a pulsed electric field before the phonon cloud builds up.²¹

²⁰ K. Nakamura and J. Yanashita, *Progr. Theoret. Phys. (Kyoto)* **39**, 545 (1968).

²¹ We are indebted to Dr. K. Nakamura for suggesting this point.

The phonon build up time is typically of the order of 10^{-9} sec, which is sufficiently long for the resonance experiment.

In order to detect the spin-orbit effects on the Γ_7 conduction band, it is desirable for ξ^2 to be as large as possible (or ω_c be as small as possible). The reasons are the following: Firstly, if ξ^2 is large, the peak structure in cyclotron resonance due to the spin-orbit effect can be seen distinctly; secondly, the combination resonance [of case (A)] and the spin resonance [of case (C)] due to the electric dipole transition can be observed; thirdly, the transverse drift velocity is small for the electric field necessary to realize case (C). In order to lower the cyclotron frequency $\omega_c/2\pi$, it is desirable to use as perfect a crystal as possible, i.e., one free from defects and impurities.

The value of ξ^2 for ZnS in Table II is nearly equal to that for CdSe, and the discussion described above for CdSe holds also for ZnS. Since the value of C for ZnS is calculated on the basis of the quasicubic model, however, the coupling parameter ξ^2 is expected to be, actually, much smaller and the drift velocity v_d , to be much larger than the calculated values. It is probably more difficult to observe the spin-orbit effect for ZnS than for CdS. It should be recalled that the discussion for CdSe is based upon the upper limit of the value of C . However, ξ^2 for CdSe is expected to be larger than that of CdS. The true value for CdSe and, hence, the possibility for observing the spin-orbit effects lie in between.

VI. SUMMARY AND CONCLUSION

The effects of crossed fields on the Γ_7 conduction band for CdS, CdSe, and ZnS may be summarized as follows:

(1) Case (A) or (C) is realized for a cyclotron frequency in the 50 GHz region. The value of ξ^2 is so small for CdS and ZnS that the spin-orbit effects must be observed by the use of spin resonance due to magnetic dipole transitions in case (C). The value of ξ^2 for CdSe is expected to be large enough to permit observing the combination resonance of case (A) and the spin resonance of case (C), due to electric and magnetic dipole transitions.

(2) In case (C), where the transverse drift velocity of an electron exceeds the velocity of sound in the crystal, phonon clouds build up around the electron to cause the broadening of the resonance line. This can be overcome by employing a pulsed transverse electric field. To estimate the effect of transverse drift motion on the line shape, $\epsilon''(\omega)$ or $\mu''(\omega)$ must be evaluated with the electron-phonon interaction taken into account.

(3) In the case of $\lambda \approx \mu$, the transverse electric field has an appreciable effect on the energy eigenvalues,

(4) but not on the transition probabilities (due to electric dipole transitions) of the additional lines which necessarily include a factor of ξ^2 .

(5) As far as the transition probabilities are concerned, the transverse electric field brings about essentially the same effect as that of rotating the external magnetic field in a plane including the c axis.

(6) Owing to the crudeness of the estimate of the values of C (except possibly for CdS), the conclusions of the discussion for the possibility of observing the spin-orbit effects remain largely arbitrary and should be taken as tentative. The detailed band-structure calculations are yet to be done for the values of C and the experimental work must be carried out along the lines described in this paper before the final conclusions can be formed.

(7) In order to carry out the resonance experiments in the lower-frequency region of ω_c , it is desirable to employ as perfect a crystal as possible.

ACKNOWLEDGMENTS

The author would like to express his deepest gratitude to Dr. H. Osafune, Dr. Y. Matukura, Dr. T. Okada, and Dr. S. Nakanuma for their continual guidance and encouragement. He also wishes to thank Professor S. Makishima and Professor S. Shionoya for valuable advice during his stay at the Institute for Solid State Physics, the University of Tokyo. Professor T. Koda's comments have been most helpful during the preparation of the manuscript. Thanks are also due to K. Kani and members of the C.A.D. (Computer Aided Design) group for numerical calculations which were carried out on a NEAC 2200 model 500 computer.

APPENDIX: METHOD FOR OBTAINING NUMERICAL SOLUTIONS

Let us write the Schrödinger equation of the reduced Hamiltonian K as follows:

$$K\psi = \epsilon\psi, \quad (\text{A1})$$

and expand the wave function ψ as a linear combination of the Landau and spin states $|n, \pm\rangle$ as

$$\psi = \sum_{n=0}^{\infty} (A_n |n, -\rangle + B_n |n, +\rangle). \quad (\text{A2})$$

Then, the secular equation to be solved is

$$\det(K - \epsilon) = 0, \quad (\text{A3})$$

where we place the base vectors in the following order:

$$|0, -\rangle, |0, +\rangle, |1, -\rangle, |1, +\rangle, \dots, |n, -\rangle, |n, +\rangle, \dots$$

By converting the phase factors of A_n and B_n as follows,

$$\begin{aligned} A_{2m} &\rightarrow iA_{2m}, \\ B_{2m+1} &\rightarrow iB_{2m+1}, \end{aligned} \quad (m=0, 1, 2, \dots)$$

the matrix K can be transformed into a real symmetric one such that

$$\begin{aligned} &\begin{pmatrix} \frac{1}{2}-\mu & -i\lambda & & & \\ i\lambda & \frac{1}{2}+\mu & -\xi & & \\ & -\xi & \frac{3}{2}-\mu & -i\lambda & \\ & & +i\lambda & \frac{3}{2}+\mu & \\ & & & & \dots \end{pmatrix} \begin{pmatrix} iA_0 \\ B_0 \\ A_1 \\ iB_1 \\ \dots \end{pmatrix} \\ &= \begin{pmatrix} \frac{1}{2}-\mu & -\lambda & & & \\ -\lambda & \frac{1}{2}+\mu & -\xi & & \\ & -\xi & \frac{3}{2}-\mu & \lambda & \\ & & \lambda & \frac{3}{2}+\mu & \\ & & & & \dots \end{pmatrix} \begin{pmatrix} A_0 \\ B_0 \\ A_1 \\ B_1 \\ \dots \end{pmatrix}. \quad (\text{A4}) \end{aligned}$$

After truncating the matrix into a finite-rank submatrix, we carried out the diagonalization by computer.